Magazine of Concrete Research, 2010, **62**, No. 3, March, 157–162
doi: 10.1680/macr.2010.62.3.157

Fracture parameters of high-strength concrete – mode II testing

C. Naga Satish Kumar and T. D. Gunneswara Rao

National Institute of Technology

This paper presents an experimental investigation on fracture parameters (fracture energy and brittleness number) of double-edge-notched, high-strength concrete specimens of different sizes with varying notch depth ratios under mode II testing. Fracture energy and brittleness number are the important parameters for modelling the fracture behaviour of concrete. The fracture parameters are calculated by using size effect law. The size effect indicates that the failure stress of geometrically similar structures decreases with increasing size. From the experimental results it is observed that shear fracture energy (G_{II}) is about 23 times more than that of mode I fracture energy (G_I). It is also observed that the cracks do not propagate from the notches in the direction normal to the maximum principal stress but in a direction in which shear stresses dominate as reported by Bazant. The crack propagation direction seems to be governed by maximum energy release rate.

Introduction

Quasi-brittle materials such as concrete exhibit moderate strain hardening prior to the attainment of ultimate tensile strength and tension softening thereafter. For an ideal brittle material, the stress–strain curve is linearly elastic up to the maximum stress, at which point an initial flaw catastrophically propagates, leading to failure. The formation of cracks in concrete marks the beginning of a serious problem in concrete structures. The fracture behaviour of quasi-brittle materials has drawn the attention of many researchers. Significant research work has been carried out in the last few decades and there is consensus among the research community to introduce fracture mechanics theory into design methodology (Bazant, 1998; Bhushan Karihaloo, 1995).

Mode II failure, the failure of structures due to in-plane shear, has received significant importance in civil engineering practices, since this failure is brittle and hence potentially catastrophic. Some practical situations where the shear cracking is predominant are: deep beams, severe concentrated loading, punching shear, penetration of projectiles into concrete, shear keys and so on. Mode II type of failure is also found in short corbels, bearing shoes, ledger beam bearings, and web flange stress transfer cases. The analysis of concrete members under shear action requires material parameters.

As far as concrete is concerned, mode I is a relatively clear type of crack propagation. So many researchers have undertaken an enormous amount of experimental and theoretical work to understand mode I fracture. However, studies on mode II loading effects are very limited for concrete. Many researchers (Bazant and Pfeiffer, 1986; Davies, 1995; Swartz and Taha, 1990) have attempted to study pure mode II fracture. Since Iosipescu's (1967) shear testing specimen is proposed, a superimposed mode I component cannot be avoided in the specimen configurations used in their experiments. In order to perform mode II fracture experiments without a superimposed mode I component, a double-edge-notched specimen is proposed and is applied to wood by Xu *et al.* (1996). Later this kind of geometry is extended to the measurement of K_{IIc} of normal-strength concrete. This specimen geometry was numerically and experimentally studied by some researchers (Reinhardt *et al.*, 1997; Reinhardt and Xu, 1998). However, fracture energy has not yet been measured. Recently Reinhardt and Xu (2000) conducted experiments on double-edge-notched concrete specimens and calculated fracture energy using work of the fracture method (G_{IIF}).

In the present paper an expression for fracture energy

Department of Civil Engineering, National Institute of Technology, Warangal 506004, India

(MACR 800145) Paper received 23 August 2008; accepted 24 July 2009

(G_{IIf}) for mode II loading based on the Bazant's size effect law (Bazant, 1984) is proposed and also a procedure to evaluate the fracture energy (G_{IIf}) of high-strength concrete from practical experiments on double-edge-notched concrete specimens is presented.

Fracture energy from the size effect law

The total potential energy of a structure can also be written as

$$U = U_s \times V \times F(\alpha)$$

where V = nominal volume of the structure $= hb2d = h^2b$ in which h is the height of the specimen, $2d$ is the width of the specimen and b is the thickness of the specimen (Figure 1); U_s = nominal strain energy density = (stress)$^2/2E = (P^2/b^2d^2)/2E$; $F(\alpha)$ = certain function of the relative crack length; $\alpha = a/d$ where a is the crack length.

The energy release rate, that is the energy released per unit thickness and unit extension of the crack length, may be calculated as

$$G = -\frac{1}{b}\frac{\partial U}{\partial a} = -\frac{1}{bd}\frac{\partial U}{\partial \alpha}$$

This yields

$$G = \frac{P^2}{Edb^2}g(\alpha) \quad (1)$$

in which $g(\alpha) = -2F'(\alpha)$ (the prime denotes derivatives), and load P is not necessarily the failure load P_u. Equation 1 is valid for the condition of plane stress.

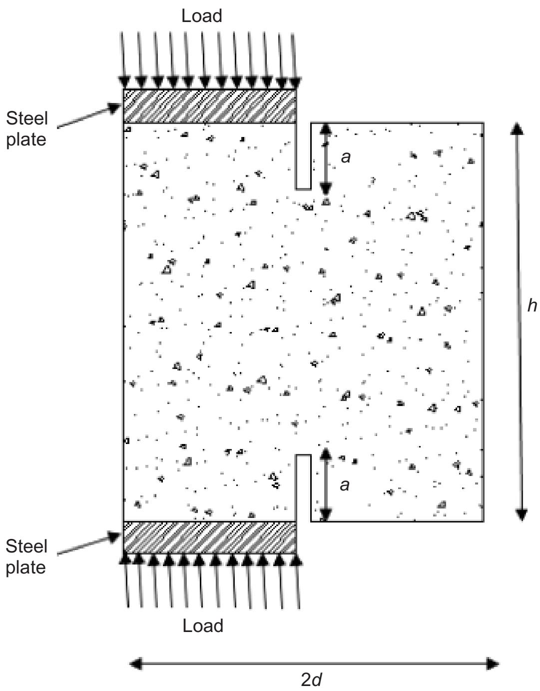

Figure 1. Details of double-edge-notched specimen for mode II failure

For the case of plane strain, E must be replaced by $E/(1-\mu^2)$ where μ is the Poisson's ratio. Function $g(\alpha)$ depends only on the specimen geometry but not on its size. In linear elastic fracture mechanics it is shown that

$$G = \frac{K_{II}{}^2}{E}$$

where K_{II} is the mode II stress intensity factor.

The stress intensity factor as per Tada's handbook (Tada *et al.*, 1985) for a double-edge-notched plate subjected to tensile force is $K_{II} = \frac{1}{4}\sigma\sqrt{d}f(\alpha)$ in which

$$f(\alpha) = \sqrt{\frac{(1-\alpha)}{(2-\alpha)}}\left[1 + 0{\cdot}5\left(\frac{1}{2-\alpha}\right) + 0{\cdot}375\left(\frac{1}{2-\alpha}\right)^2 - 1{\cdot}081\left(\frac{1}{2-\alpha}\right)^3 + 5{\cdot}580\left(\frac{1}{2-\alpha}\right)^4 - 4{\cdot}061\left(\frac{1}{2-\alpha}\right)^5\right]$$

and $\sigma = P/bd$

Thus Equation 1 is equivalent to

$$\frac{1}{16}\frac{P^2}{b^2d^2}d[f(\alpha)]^2\frac{1}{E}$$

$$\frac{1}{16}\frac{P^2}{b^2d^2}d[f(\alpha)]^2\frac{1}{E} = \frac{P^2}{Edb^2}g(\alpha)$$

$$g(\alpha) = \frac{1}{16}[f(\alpha)]^2 \quad (2)$$

The crack propagates when K_{II} reaches the fracture toughness K_{IIc}, or G reaches the fracture energy R required for further crack growth, $R = K_{IIc}{}^2/E$. As proposed by Bazant (1987), the fracture energy G_f may be uniquely defined as the energy required for crack growth in an infinitely large specimen. Then, considering the limit $d \to \infty$ and $\alpha \to \alpha_0$ where $\alpha_0 = a_0/d$, a_0 is the notch length or initial crack length, then

$$G_f = \text{Lim}_{d\to\infty} R = \text{Lim}_{d\to\infty}\frac{P_u{}^2}{Edb^2}g(\alpha) \quad (3)$$

Substituting P_u according to the size effect law yields

$$\sigma_N = Bf_t\left(1 + \frac{d}{d_0}\right)^{-1/2}$$

$$P_u{}^2 = B^2f_t{}^2b^2d\left(\frac{d}{1+(d/d_0)}\right) \quad (4)$$

Substituting $P_u{}^2$ into Equation 3 gives

$$G_f = \frac{B^2f_t{}^2}{E}g(\alpha_0)d_0 \quad (5)$$

The size effect law proposed by Bazant can be algebraically transformed to a linear regression equation, $Y = C + AX$ in which $Y = (f_t/\sigma_N)^2$, $d_0 = C/A$ and

$B = C^{-1/2}$. Substituting d_0 and B values into Equation 5 yields

$$G_f = \frac{f_t^2}{AE} g(\alpha_0) \qquad (6)$$

For infinitely large specimens Bazant and Kazemi (1990) have proposed the fracture process zone length and brittleness number as

$$C_f = \frac{g(\alpha_0)}{g^1(\alpha_0)} d_0$$

Brittleness number

$$\beta = \frac{g(\alpha_0)}{g^1(\alpha_0)} \frac{d_0}{C_f} = \frac{d}{d_0}$$

where

$$g^1(\alpha) = \frac{dg(\alpha_0)}{d(\alpha_0)} = \frac{1}{8}\left[f^1(\alpha_0)\right]$$

Experimental programme

Material details

Ordinary Portland cement (OPC) of 53 grade conforming to ASTM C150 type 1 with specific gravity of 3·15 was used in the concrete mix; natural river sand with specific gravity 2·60 meeting the requirements of ASTM C-33 was also used as fine aggregate in the investigation. Crushed coarse aggregate passing through a 20 mm sieve and retained on a 10 mm sieve (60%) and retained on a 4·75 mm sieve (40%) with specific gravity 2·7 was used. To achieve the desired workability CONPLAST SP337 was used as superplasticiser. The dosage of superplasticiser was 40 ml/kg (by weight of binder). Ten per cent of weight of cement was replaced by ground granulated blastfurnace slag (GGBS). The details of mix proportions are given in Table 1.

Casting

Cubes of 100 mm size were used to determine the compressive strength of concrete. Cylinders with 150 mm diameter and 300 mm length were used to determine the splitting tensile strength of concrete. Prisms of 100 mm × 100 mm × 400 mm size were adopted to determine the modulus of rupture. Specially prepared wooden moulds were used for casting the double-edge-notched concrete specimens. A needle vibrator was used for compaction. All the specimens were water cured for 28 days. After the curing period, the test specimens were dried and provided with a notch of depth conforming to notch depth ratios of 0·16, 0·2 and 0·25 by using a concrete cutter. The specimen sizes used in the present study are shown in Table 2. In this experimental investigation a total of 27 double-edge-notched concrete specimens were cast.

Test set-up and testing procedure

A Tinius Olsen testing machine (TOTM) of 4 00 000 lb (1779 kN) capacity was used for the testing of specimens. After 28 days of curing the samples were taken out from the curing tank and kept for drying for 24 h. After this the sample was coated with whitewash. One day later the sample was kept for testing. One steel plate of width up to crack distance from the edge of the specimen was kept at the centre of the TOTM platform and the sample was placed on the steel plate. Another steel plate was kept above the sample and the TOTM top platform was lowered. The specimens were subjected to compressive loading in a displacement-controlling loading machine under a constant displacement rate of 0·1 mm/min; the load increased while the two

Table 1. Mix proportions of concrete mix (M70)

Cement: kg/m^3	Fine aggregate: kg/m^3	Coarse aggregate: kg/m^3	GGBS: kg/m^3	Water/binder ratio	Superplasticiser: ml/kg
600·0	580·0	1080·0	65·0	0·25	40·0

Table 2. Details of double-edge-notched specimens

Crack depth ratio	Specimen designation	Size of the specimens: $h \times 2d \times b$	No. of samples
$a/h = 0{\cdot}16$	H/75/0·16	75 × 75 × 75	3
	H/150/0·16	150 × 150 × 75	3
	H/300/0·16	300 × 300 × 75	3
$a/h = 0{\cdot}20$	H/75/0·2	75 × 75 × 75	3
	H/150/0·2	150 × 150 × 75	3
	H/300/0·2	300 × 300 × 75	3
$a/h = 0{\cdot}25$	H/75/0·25	75 × 75 × 75	3
	H/150/0·25	150 × 150 × 75	3
	H/300/0·25	300 × 300 × 75	3

mode-II cracks extended and new cracks were generated in the compressed part of the specimen. Finally, the compressive load at the specimens that failed by vertical splitting or diagonal shear was recorded. Figure 1 shows the schematic arrangement of the double-edge-notched specimen subjected to compressive loading.

To ascertain the mechanical properties of concrete, five companion cubes, five companion cylinders and five companion prisms were cast and tested on the TOTM. The average values of the mechanical properties of concrete are given in Table 3.

Test results and discussions

All the double-edge-notched, high-strength concrete specimens were also on the TOTM under displacement rate control. To determine the fracture parameters with the help of the size effect method, linear regression plots were prepared and are presented in Table 4. The linear regression plots consisted of $(f_t/\sigma_N)^2$ on the Y-axis and size (d) on the X-axis. The regression equation is in the form of $Y = C + AX$. The characteristic size of the tested beams is reported as $d_o = C/A$ and the numerator in the size effect law $B = C^{-1/2}$. f_t is the direct tensile strength of concrete. In the absence of direct tensile test the value f_t is taken as 0·665 times the split tensile strength of concrete (Neville, 1995). The fracture energy and brittleness number were determined with the help of the size effect method and reported in Table 5.

During the tests, the crack propagation of all the specimens was carefully observed. A shear crack started at the tip of the notch when the loading reached a certain value, then the crack propagated along the ligament and finally unloaded part of the specimen slides with respect to the loaded part of the specimen. In some specimens it was observed that the crack propagation trajectory was curved owing to the influence of the randomly distributed particles of coarse aggregates in concrete. A photograph of the tested samples is shown in Figure 2.

The fracture energy determined is the mean prediction for a particular notch depth ratio. With the help of Equation 5, it can be observed that for a given double-edge-notched specimen, the fracture energy is inversely

Table 3. Mechanical properties of concrete

Cube compressive strength: N/mm^2	Split tensile strength: N/mm^2	Modulus of rupture: N/mm^2
83·06	6·67	7·52

Table 4. Peak load and nominal stress of tested specimens

Crack depth ratio	Specimen designation	Load: kN (P)	Nominal stress: N/mm^2 (σ_N)	$\left(\frac{f_t}{\sigma_N}\right)^2$	d: mm
$a/h = 0{\cdot}16$	H/75/0·16	225·29	80·103	0·003086	37·5
	H/150/0·16	425·67	75·674	0·003458	75
	H/300/0·16	720·57	64·050	0·004827	150
$a/h = 0{\cdot}20$	H/75/0·2	169·91	60·412	0·005426	37·5
	H/150/0·2	315·80	56·142	0·006283	75
	H/300/0·2	529·31	47·049	0·008946	150
$a/h = 0{\cdot}25$	H/75/0·25	141·00	50·133	0·007879	37·5
	H/150/0·25	263·32	46·812	0·009036	75
	H/300/0·25	436·34	38·785	0·013100	150

Table 5. Fracture energy and brittleness number of tested specimens of different notch depth ratios

Crack depth ratio	Specimen designation	$f(\alpha_o)$	$g(\alpha_o)$	G_f: N/mm	$\beta = \frac{d}{d_0}$
$a/h = 0{\cdot}16$	H/75/0·16	0·9900	0·0612	1·812	0·2497
	H/150/0·16				0·4990
	H/300/0·16				0·9990
$a/h = 0{\cdot}20$	H/75/0·2	0·9845	0·0605	0·896	0·2931
	H/150/0·2				0·5862
	H/300/0·2				1·1720
$a/h = 0{\cdot}25$	H/75/0·25	0·9674	0·0584	0·576	0·3095
	H/150/0·25				0·6190
	H/300/0·25				1·2380

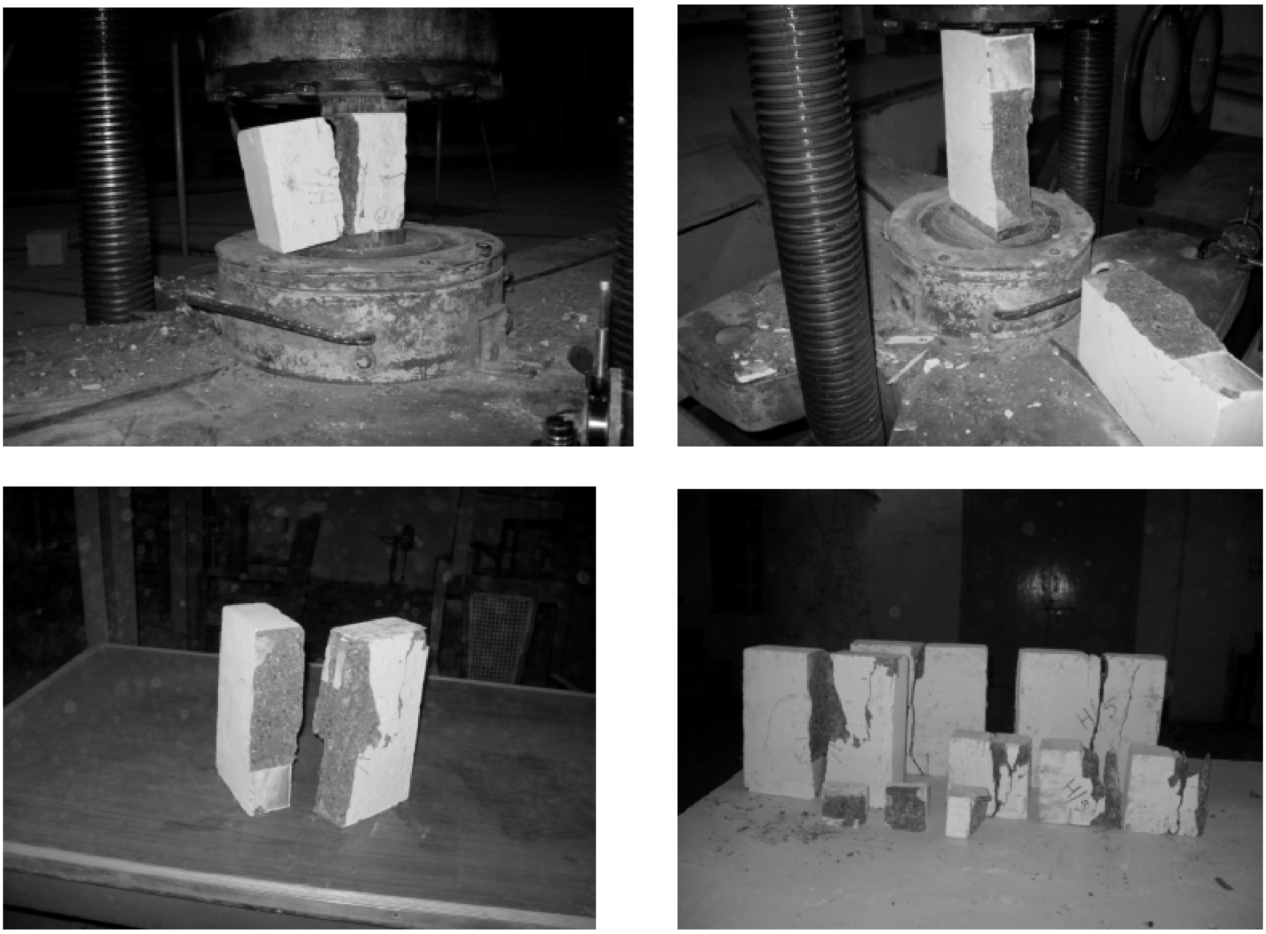

Figure 2. Tested double-edge-notched specimens

proportional to the slope of the regression line. In the present investigation, it is found that the slope of the regression line (A) increased with the increase in the notch depth ratio. This indicates that the increase in notch depth ratio decreases the fracture energy.

The brittleness number as indicated by $\beta = d/d_0$ characterises the brittleness of the member. For $0{\cdot}1 < \beta < 10$, the non-linear fracture mechanics should be used (Einsfeld and Marta, 2006). Quasi-brittle structures (RILEM Technical Committee QFS, 2004) are those for which $0{\cdot}1 \leqslant \beta \leqslant 10$. If $\beta < 0{\cdot}1$, then the failure may be analysed on the basis of the strength criterion and if $\beta > 10$, then the failure may be analysed according to the linear elastic fracture mechanics (LEFM) (Bazant *et al.*, 1986). In the present study, an increase in the notch ratio decreased the characteristic dimension d_o thereby increasing the brittleness of the member. In other words, it can be stated that an increase in the crack length (owing to external forces) increases the brittle number (brittleness) of the element. Thus brittleness of concrete depends more on the size or length of the crack. Figure 3 shows the variation of brittleness number with the notch depth ratios.

From Table 5, it is observed that the fracture energy for mode II failure is in the range 570–1800 N/m of different notch depth ratios. This value is approximately 23 times more than the tensile (mode I) fracture energy (the range of G_1 is 25–80 N/m) (Vidyasagar *et al.*, 2005). This large difference can probably be explained by the fact that shear fracture energy includes not only the energy to create inclined tensile microcracks in the fracture process zone but also the energy required to break the shear resistance owing to interlock of aggregate.

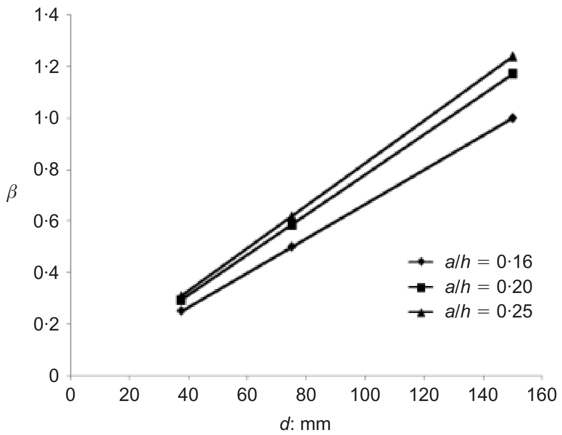

Figure 3. Brittleness number 'd' curves for different notch depth ratios

The present study has yielded the fracture parameters of high-strength concrete under mode II testing. The fracture parameters are essential for the design of concrete structures to have economical as well as more accurate detailing. The size effect method provides a relatively easy way by which to obtain the fracture parameters by measuring the peak load only. The material properties under mode II loading are needed for analysis of shear problems of beams and slabs.

Conclusions

Based on the tests on 27 double-edge-notched, high-strength concrete specimens, the following conclusions can be drawn.

(*a*) The results have shown that by measuring the peak loads it is possible to obtain the fracture parameters under mode II loading without resorting to sophisticated measurements.
(*b*) Like the tensile fracture (mode I), the shear fracture (mode II) also follows the size effect law.
(*c*) The fracture energy increases with decrease in *a/h* ratio; that is, the fracture energy increases as the crack depth decreases.
(*d*) The brittleness number increases with *a/h* ratio.
(*e*) The fracture energy in mode II failure is 23 times more than the mode I failure.

Acknowledgement

The authors are very thankful to the authorities of the National Institute of Technology, Warangal, for providing facilities for carrying out this work.

References

Bazant ZP (1984) Size effect in blunt fracture: concrete, rock and metal. *Journal of Engineering Mechanics, ASCE* **110(6)**: 1336–1355.

Bazant ZP (1987) SEM/RILEM. *International Conference on Fracture of Concrete and Rock*. Society for Experimental Mechanics, Bethnel, CT, pp. 390–402.

Bazant ZP (1998) *Fracture and Size Effect in Concrete and Other Quasibrittle Materials*. CRC Press, Boca Raton.

Bazant ZP and Kazemi T (1990) Determination of fracture energy, process zone length and brittleness number from size effect, with application to rock and concrete. *International Journal of Fracture* **44(2)**: 111–131.

Bazant ZP and Pfeiffer PA (1986) Shear fracture tests of concrete. *Materials and Structures* **19(110)**: 111–121.

Bazant ZP, Jin KK and Pfeiffer PA (1986) Nonlinear fracture properties from size effect tests. *Journal of Structural Engineering* **112(2)**: 289–306.

Bhushan Karihaloo L (1995) *Fracture Mechanics and Structural Concrete*. Longman Scientific and Technical.

Davies J (1995) Study of shear fracture in mortar specimens. *Cement and Concrete Research* **25(5)**: 1031–1042.

Einsfeld RA and Marta SLV (2006) Fracture parameters of high performance concrete. *Cement and Concrete Research* **36(3)**: 576–583.

Iosipescu N (1967) New accurate procedure for single shear testing of metals. *Journal of Materials* **2(3)**: 537–566.

Neville AM (1995) *Properties of Concrete*, 4th (final) edn. Pearson Education, Delhi.

Reinhardt HW and Xu S (1998) Experimental determination of K_{IIc} of normal strength concrete. *Materials and Structures* **31(5)**: 296–302.

Reinhardt HW and Xu S (2000) A practical testing approach to determine mode II fracture energy G_{IIF} for concrete. *International Journal of Fracture* **105(2)**: 107–125.

Reinhardt HW, Ozbolt J, Xu S and Dinku A (1997) Shear of structural concrete members and pure mode II testing. *Advanced Cement Based Material* **5(3)**: 75–85.

RILEM Technical Committee QFS (2004) Quasi-brittle fracture scaling and size effect: final report. *Materials and Structures* **37(8)**: 547–568.

Swartz SE and Taha NM (1990) Mixed mode crack propagation and fracture in concrete. *Engineering Fracture Mechanics* **35(1)**: 137–144.

Tada H, Paris and Irwing R (1985) *The Stress Analysis of Crack Handbook*, 2nd edn. Paris Productions.

Vidyasagar R, Dinesh SV and Santosh AC (2005) Fracture energy of normal and HSC beams. *The Indian Concrete Journal* November 37–42.

Xu S, Reinhardt HW and Gappoev M (1996) Mode II fracture testing method for highly orthotropic materials like wood. *International Journal of Fracture* **75(3)**: 185–214.

Discussion contributions on this paper should reach the editor by 1 September 2010